Published on 19 July 2013. Downloaded by Changchun Institute of Optics, Fine Mechanics and Physics, CAS on 17/03/2014 01:06:29.

PCCP

RSC Publishing

PAPER

View Article Online
View Journal | View Issue

Evanescent field excited plasmonic nano-antenna for improving SERS signal†

Cite this: *Phys. Chem. Chem. Phys.*, 2013, **15**, 15494

Yuejiao Gu,[a] Haibo Li,[a] Shuping Xu,[a] Yu Liu[b] and Weiqing Xu*[a]

Received 21st June 2013,
Accepted 18th July 2013

DOI: 10.1039/c3cp52581c

www.rsc.org/pccp

The purpose of this work is to develop a high-performance surface-enhanced Raman scattering (SERS) substrate with high light harvesting and SERS emitting efficiencies based on the principle of a plasmonic nano-antenna. A prism/Ag nanowell array was designed and constructed based on the Kretschmann configuration. Almost 100% of the incident light can be absorbed at the resonance angle. A strong electromagnetic (EM) field is generated in the near field along the rim and at the center of the nanowells by means of the localized energy of surface plasmons (SPs), resulting in the electric field being enhanced 300 times at the Ag surface. The co-enhancement of localized SPs and propagating SPs was achieved in this substrate. The plasmonic nano-antenna structure can also redirect the SERS, which benefits the SERS collection. The SERS sensitivity on this configuration was improved by about 40 times compared with that on a conventional Kretschmann configuration with a flat Ag film. This SERS substrate design with full consideration on the tuning of the EM field in the near field and SERS space distribution in the far field could give insight into the design of a new generation of SERS substrates.

I. Introduction

Surface-enhanced Raman scattering (SERS) spectroscopy is a noninvasive optical spectroscopy method that is capable of providing detailed information about molecular structure.[1] The enhancement capacity is essential for its application as a sensitive detection tool. In the enhancement of SERS, the absorption and scattering cross section of nanostructures plays a critical role. So the effective coupling of surface plasmons (SPs) is considered to be a key point.[2–4] The strategies involve the localized surface plasmon resonance (LSPR)-coupled and propagating surface plasmon resonance (PSPR)-coupled modes. For the LSPR-coupled strategy, the LSPR bands and the excited light were required to be well matched.[5,6] The cross sections of the absorption and scattering of the nanoparticles and nanoaggregates are very small (about 10^{-15} m^2),[7] which indicates that the majority of the incident light could not be harvested for the usual LSPR-coupled SERS substrates. Increasing the absorption cross sections of the nanostructures can improve the enhancement of SERS.[8] To best couple SPs, many optical configurations and devices were designed in combination with the PSPR-coupled strategy, such as prism,[9–11] waveguide[12] and grating[13,14] configurations. Compared with other coupling configurations, the prism configuration can easily achieve the coupling of SPs by means of modulating the incident wave vector to match the SP wave vector *via* tuning of the incident angle. A high coupling efficiency approaching 100% can be obtained at the resonance angle. The effective coupling of SPs guarantees a suitably high collection of the incident light energy.

The prism coupling is based on a well-established SPR spectroscopy method with Kretschmann (KR) configuration, which is commercially available. In recent years, the KR configuration has been developed for the simultaneous detection of SPR and SERS.[9,15–17] However, its application is limited owing primarily to weak SERS intensities recorded in a KR configuration. It is because the propagating SPs (PSPs) on a smooth metal film only support a weak electromagnetic (EM) field.[18] Hence the key issue lies in the utilization of the collected energy to enhance the SERS signal.

Recently, plasmonic antennas, such as nanorods,[19] bow-ties,[20] nano arrays[21,22] *etc.*, have attracted researchers due to their distinguished capacity for light control. Plasmonic antennas are considered to be the bridge of the far field and the near field optics, which allows focusing of the propagating light to the near field and emitting the near field energy to the far field

[a] *State Key Laboratory of Supramolecular Structure and Materials, Jilin University, Changchun 130012, P. R. China. E-mail: xuwq@jlu.edu.cn; Fax: +86-431-85193421; Tel: +86-431-85168505*

[b] *State Key Laboratory of Applied Optics, Changchun Institute of Optics, Fine Mechanics and Physics, Chinese Academy of Sciences, Changchun, 130033, P. R. China*

† Electronic supplementary information (ESI) available: (1) Relation between the wave vector of the excited PSP with a prism and that of the output process with an Ag nanowell array. (2) Setup of the device for measuring SERS spectra in an evanescent field excitation. (3) The details of the FDTD simulation. (4) Setup for measuring the angle-resolved SERS spectra. (5) SERS space distribution. See DOI: 10.1039/c3cp52581c

This journal is © the Owner Societies 2013

Published on 19 July 2013. Downloaded by Changchun Institute of Optics, Fine Mechanics and Physics, CAS on 17/03/2014 01:06:29.

efficiently.[23,24] Since the SERS enhancement capability is closely related to the absorption and scattering cross section of nanostructures, it can also be improved by the principle of plasmonic nano-antennas. In this paper, a nano-antenna analogue involving a prism/Ag nanowell array was proposed. By using the KR configuration, a high light harvesting efficiency approaching 100% was achieved. The employment of a nanowell array can concentrate the energy harvested to the local field, which generates a 300 times enhancement of the EM field. Also, the nanowell array can redirect the SERS,[25,26] which benefits the SERS collection. The finite-difference time-domain (FDTD) method was used to help us understand the SERS radiation pattern on this SERS antenna structure.

II. Experimental section

The nanosphere lithography method was adopted to construct the periodic structure.[22] To be specific, a close-packed 680 nm-diameter polystyrene (PS) nanosphere monolayer (PS nanosphere was prepared by following the literature method[27]) was assembled on a BK7 glass slide by an interface method.[28] The PS nanosphere monolayer was etched with oxygen reactive ion etching (Plasmalab 80Plus, Oxford Instruments) to reduce the size of the PS nanospheres. An Ag film (thickness defined as h_2, shown in Fig. 1) was deposited on the PS nanosphere monolayer by vacuum evaporation (Beijing Technol Science Co. Ltd., China). The PS nanospheres were removed using ultrasonication in methanol. Finally a Ag film (thickness defined as h_1, shown in Fig. 1) was deposited to form the periodic Ag nanowell structure. The morphology was characterized by scanning electron microscopy (SEM, JEOL JSM-6700F). The period (Λ) of the nanowell array was controlled by the diameter of the PS spheres and $\Lambda = \sqrt{3}/2 \times D$ (D is the diameter of the PS spheres). Since PS spheres of 680 nm were used, the Λ of the array was 590 nm.

A Raman probe, 4-aminothiophenol (4-ATP), was immobilized on the prepared periodic structure. The slides were immersed in a 4-ATP ethanol solution (1.0×10^{-4} mol L^{-1}) for 30 min and rinsed with water. Slides with a flat Ag film were also assembled with 4-ATP as a contrast.

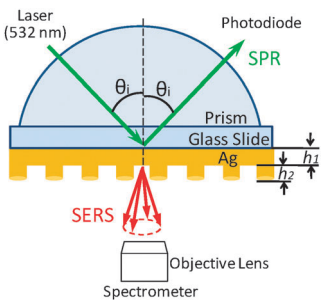

Fig. 1 Schematic of the plasmonic nano-antenna with a prism/Ag nanowell array structure. SERS is collected at the air side below the prism using an objective lens. h_1 and h_2 indicate the thickness of the Ag film and the height of the nanostructure respectively.

In the experiment, the slide was coupled to the bottom surface of a semi-cylindrical prism by an index matching fluid (refractive index = 1.515, Shanghai Specimen and Model Factory, China).

III. Results and discussion

1. The design of the plasmonic nano-antenna configuration by evanescent field excitation for SERS detection

Fig. 1 shows the designed plasmonic nano-antenna with high light harvesting and SERS emitting efficiencies. There are two key points in the design of the nano-antenna: energy harvesting (coupling light from the far field to the near field) and energy emitting (the near field to the far field). In the present study, the energy harvesting process was completed using a prism. As we previously stated, its coupling efficiency was almost 100%. The SPs propagating on the metal film can be localized at the rim of the nanostructures, forming an enhanced EM field by localized SPs (LSPs), which contributes to a strong SERS signal. To control the emission process of the SERS, a metallic periodic structure analogous to the phase-array antennas was designed. This structure can tune the light radiation pattern. (The relationship between the wave vectors of the SPs and light on this model is analyzed in part 1 of the ESI.†) It is known that SPs propagating on a periodic metal surface will couple to light, and the decoupled light will directionally radiate into space.[29] It is beneficial to improve the collection efficiency of the SERS.

2. The optimization of the parameters of the SERS substrates

2.1 The optimization of the period of the Ag nanowell array for high SERS collection efficiency. To get a SERS substrate with high performance, the SP characteristics of the metal structure should be carefully designed and validated. First, the period of the Ag nanowell array should be determined, because it can influence the out-coupling emission angle of the SERS signal. The SEM image of the Ag nanowell array as the SERS substrate is shown in Fig. 2(a). It was found that the nanowell array is

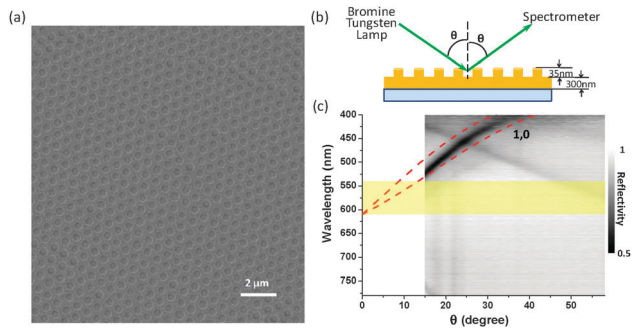

Fig. 2 (a) SEM image of the prepared periodic Ag nanowell constructed by the nanosphere lithography and the reactive ion etching method. (b) Schematic diagram for recording the angle-dependent reflection spectra. A bromine tungsten lamp and a spectrometer were used as light source and detector. (c) The angle-dependent reflection spectra of the periodic Ag nanowell. Dashed lines show the calculated resonance conditions according to the Bragg scattering equation. The highlighted region indicates the Raman shift range of 0–2400 cm^{-1} under 532 nm excitation.

Published on 19 July 2013. Downloaded by Changchun Institute of Optics, Fine Mechanics and Physics, CAS on 17/03/2014 01:06:29.

uniform over a relatively large area. Fig. 2(b) and (c) present the detection schematic diagram and the detection results of angle-dependent reflection spectra using a 590 nm period Ag nanowell array. The minimum reflectivity strip (shown as the dark area) is the dominant resonance mode, which belongs to the (1,0) Bragg mode. The resonance angles are in accordance with the calculation results by using the Bragg scattering equation.[30] We tuned the resonance wavelength at a small angle (<10 degrees) to match the Raman shift range (the light yellow range shown in Fig. 2(c)), which means that the SERS signal can be out-coupled at small divergence angles for easy collection. That is the reason why we chose 590 nm as the period of the array.

2.2 The optimization of the Ag nanowell array for high light excitation efficiency. The effective coupling of the incident light into SPs on the Ag periodic structure in KR configuration is a fundamental problem. In the present study, the coupling was optimized from two aspects, the physical factors of the nanowells and the incident angle. In order to obtain the deepest and sharpest SPR curve, the Ag film thickness (h_1) and the periodic structure height (h_2) (as shown in Fig. 1) were optimized, because they are both closely related to the radiation damping of SPs (the relationship of the radiation and the internal damping of the SPs determines the resonance depth of the SPR.[22]). Fig. 3(a) shows the SPR curves of the periodic structure under different h_1 and h_2. The sharpest SPR reflectivity was observed when h_1 = 25 nm and h_2 = 35 nm. Fig. 3(b) shows the incident angle-dependent SERS spectra of 4-ATP on the Ag periodic structure measured by collecting the SERS signal below the prism as shown in Fig. 1. More details about the setup of the device are provided in part 2 of the ESI.† Fig. 3(c) shows the SPR curve and the plot of SERS intensities at 1436 cm^{-1} at different incident angles. The maximum SERS intensity was obtained at 45.2°, which is accordant with the resonance angle. It is about 35 times higher compared to non-resonance conditions (*e.g.* 54°).

3. Evaluation the SERS enhancement on KR configuration with Ag nanowell array

3.1 The EM field enhancement in the near field. A strong interaction between PSPs and LSPs is anticipated in the presence of nanostructures on the KR configuration. In the light input process the addition of an Ag nanowell array perturbs the PSPs.

Another kind of SPs, the LSPs, formed due to the crimpling of the surface, which would greatly enhance the local EM fields. Fig. 4 shows the electric field distribution of the periodic structure in the near field (simulated using Lumerical FDTD Solutions software, Canada, more details of the simulation model can be found in part 3.1 of the ESI†). It was found that the energy of SPs propagating on the metal surface can be localized along the rim and at the center of the Ag nanowells. The electric field by means of LSPs increases by about 300 times along the rim and 240 times at the center of the Ag nanowells. It is much improved when compared with the PSPs dominated flat metal film on which the EM field is only enhanced by about a dozen times.[31] The high enhancement of the EM field could guarantee a high SERS enhancement. It should be noted that the intensity of LSPs is closely related to the intensity of PSPs. The EM intensity in the nanowell is very low at non-resonance angles as shown in Fig. 4(c). It indicates that the LSPs and PSPs may excite each other in this structure.

3.2 The SERS radiation pattern in the far field. The SERS space distribution was investigated using the angle-resolved spectra which were obtained by the self-made angle-resolved spectrometer. More details about this setup and how it works are provided in part 4 of the ESI.† The incident angle was set as 45.2° (the resonance angle). Different from the usual SERS detection instrument with an objective lens with large numerical aperture (NA), the NA of the collection objective lens is 0.03, which only covers about a 3.5° divergence angle and provides a high angle resolution.

Fig. 5(a) illustrates how to measure the angle-resolved SERS spectra, and the results are shown in Fig. 5(b). The spatial distributions of the SERS intensities of 4-ATP at 1145 and 1436 cm^{-1} were obtained from the angle-resolved spectra. A symmetrical emission pattern was observed with the center axis perpendicular to the substrate plane. It matches with the FDTD simulation results very well (Fig. 5(c)). We can infer that the SERS is focused in a small region around the normal axis of the substrate plane

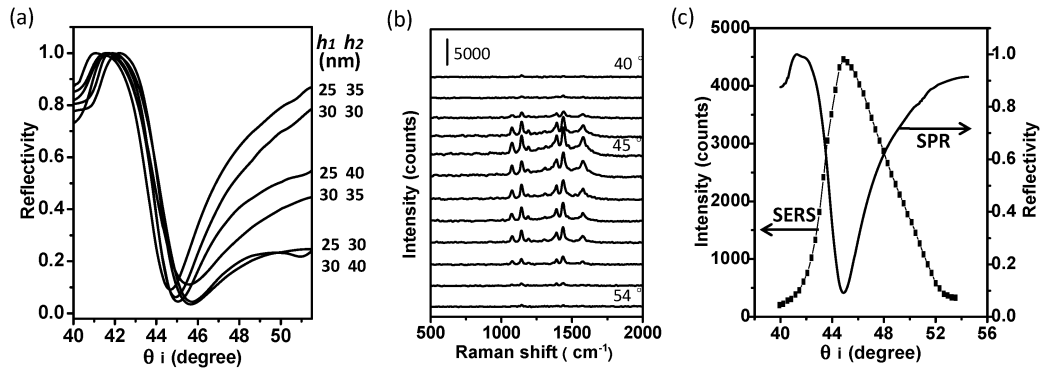

Fig. 3 (a) The angle-dependent SPR curves at 532 nm with different thicknesses of the Ag film (h_1) and different heights of the periodic structure (h_2). (b) The incident angle-dependent SERS spectra of 4-ATP on the Ag periodic structure (h_1 = 25 nm and h_2 = 35 nm) recorded at the air side below the prism by the setup in Fig. 1. Top to bottom curves correspond to the SERS spectra recorded under the incident angle of 40–54°. (c) SPR curve of the Ag periodic structure and the plot of the SERS intensity of 4-ATP (at 1436 cm^{-1}) on this substrate with varying incident angle.

 This journal is © the Owner Societies 2013

Published on 19 July 2013. Downloaded by Changchun Institute of Optics, Fine Mechanics and Physics, CAS on 17/03/2014 01:06:29.

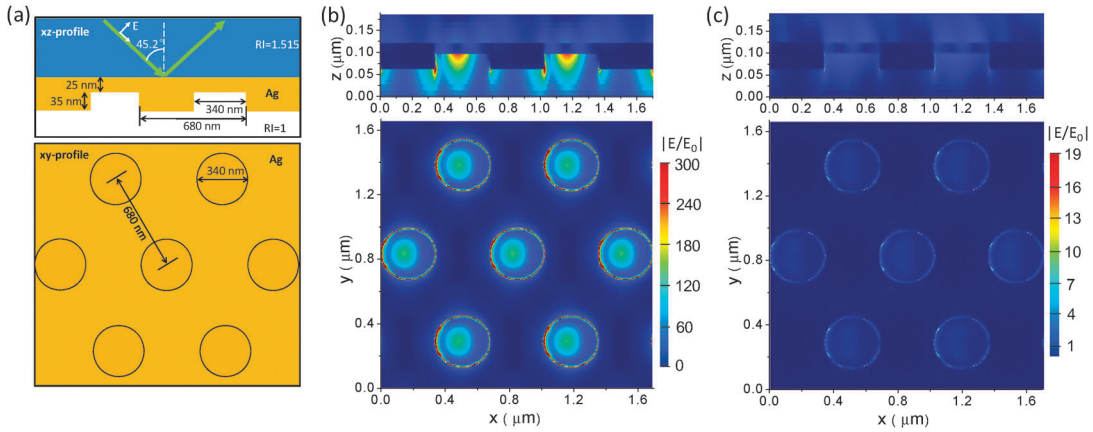

Fig. 4 (a) Schematic diagram of the calculated model for the FDTD simulation. (b) and (c) The EM field distribution on the Ag periodic structure obtained by the FDTD simulation at resonance incident angle (45.2°) and non-resonance incident angle (60°).

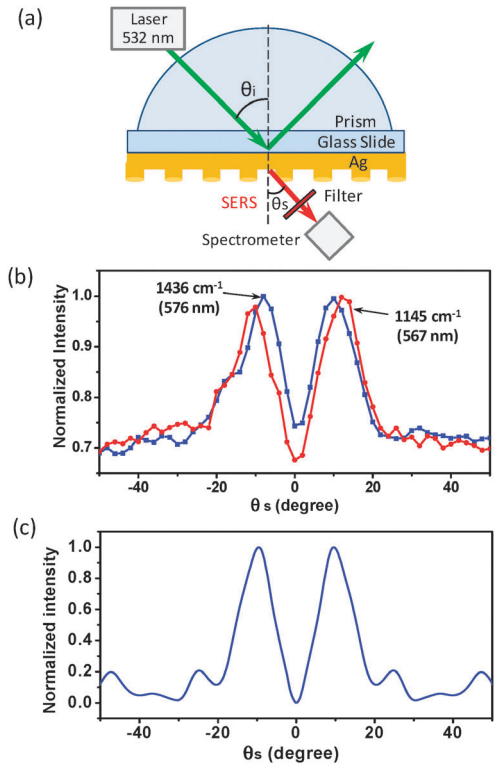

Fig. 5 (a) Schematic illustration of the setup for the angle-resolved SERS spectra on the designed periodic structure. (b) Angle-resolved SERS intensities of 4-ATP at 1145 and 1436 cm^{-1}. The NA of the objective lens is about 0.03. (c) The FDTD simulation result of the space distribution of SERS at 1436 cm^{-1}, the simulation model is shown in part 3.2 of the ESI.†

with a half-divergence angle of about 10°, which is favorable for the collection of SERS, even using a small NA objective lens.

It should be noted that, in the configuration here, there are two emission approaches of the SPs according to the theory of SP-coupled emission (SPCE). One is the directional emission at the air side through the periodic structure,[22] and the other is the directional emission at the prism side by the evanescent field.[17] Due to the scattering of the PSPs caused by the Ag periodic structure, the SERS intensity at the air side is much stronger than that at the prism side in the configuration used here (see part 5 in the ESI†).

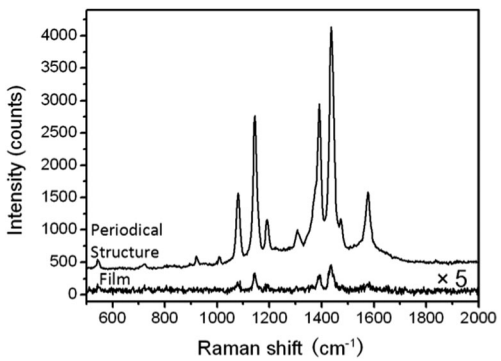

Fig. 6 SERS spectra of 4-ATP on two kinds of SERS substrates recorded at the resonance angle. Top: the Ag periodic structure; bottom: a 45 nm Ag film. The SERS intensities on the Ag film were multiplied by 5 times.

4. SERS performance compared with the traditional KR configuration

Fig. 6 shows the SERS spectra of 4-ATP on the periodic structure in the KR configuration. For comparison, the SERS spectrum of 4-ATP in a conventional KR configuration with a flat Ag film was also measured at the resonance condition. The SERS signal on the periodic structure is enhanced by about 40 times compared with on a flat Ag film. The amplified SERS signal originates from the enhancement of the EM field on the Ag periodic structure and the increase of the collection efficiency.

IV. Conclusion

In summary, an effective SERS substrate with a prism/Ag nanowell array structure was designed based on the principle of the plasmonic nano-antenna. The KR configuration was used to couple the far field energy to SPs with high efficiency. A strong EM field is generated along the rim and at the center

Published on 19 July 2013. Downloaded by Changchun Institute of Optics, Fine Mechanics and Physics, CAS on 17/03/2014 01:06:29.

of the nanowells by localizing the energy of SPs in the near field. The periodic structure tunes the SERS emission to a desired angle in the far field. Angle-resolved SERS spectra prove that the SERS signal is emitted vertically to the substrate plane with a half-divergence angle of about 10°, which facilitates the signal collection. The enhancement of SERS was about 40 times stronger compared with the usual KR configuration with a flat Ag film. The design of this SERS substrate with full consideration of the tuning of the EM field in the near field and the space distribution of SERS in the far field should give some insight into the design of a new generation of SERS substrates. In addition, the key of this SERS substrate is to improve the light harvesting and emitting efficiencies. Therefore, this model also has great potential in a broad range of applications in the design of optical elements, such as organic solar cells, nonlinear optical elements and light emitting devices, *etc*.

Acknowledgements

This work was supported by the National Natural Science Foundation of China NSFC Grant Nos. 20903043, 20973075, 21073073 and 91027010, the Research Fund for the Doctoral Program of Higher Education of China Grant No. 20090061120089 and the National Instrumentation Program (NIP) of the Ministry of Science and Technology of China No. 2011YQ03012408.

References

1 A. M. Schwartzberg, C. D. Grant, A. Wolcott, C. E. Talley, T. R. Huser, R. Bogomolni and J. Z. Zhang, *J. Phys. Chem. B*, 2004, **108**, 19191.
2 M. Moskovits, *Rev. Mod. Phys.*, 1985, **57**, 783.
3 P. Johansson, H. X. Xu and M. Käll, *Phys. Rev. B: Condens. Matter Mater. Phys.*, 2005, **72**, 035427.
4 G. C. Schatz, M. A. Young and R. P. Van Duyne, *Top. Appl. Phys.*, 2006, **103**, 19.
5 A. D. McFarland, M. A. Young, J. A. Dieringer and R. P. Van Duyne, *J. Phys. Chem. B*, 2005, **109**, 11279.
6 R. A. Álvarez-Puebla, *J. Phys. Chem. Lett.*, 2012, **3**, 857.
7 P. K. Jain, K. S. Lee, I. H. El-Sayed and M. A. El-Sayed, *J. Phys. Chem. B*, 2006, **110**, 7238.
8 E. C. Le Ru, E. Blackie, M. Meyer and P. G. Etchegoin, *J. Phys. Chem. C*, 2007, **111**, 13794.
9 Y. Liu, S. P. Xu, B. Tang, Y. Wang, J. Zhou, X. L. Zheng, B. Zhao and W. Q. Xu, *Rev. Sci. Instrum.*, 2010, **81**, 036105.
10 Y. Liu, S. P. Xu, H. B. Li, X. G. Jian and W. Q. Xu, *Chem. Commun.*, 2011, **47**, 3784.
11 X. Y. Xuan, S. P. Xu, Y. Liu, H. B. Li, W. Q. Xu and J. R. Lombardi, *J. Phys. Chem. Lett.*, 2012, **3**, 2773.
12 Y. Zhang, C. Gu, A. M. Schwartzberg and J. Z. Zhang, *Appl. Phys. Lett.*, 2005, **87**, 123105.
13 A. Kocabas, G. Ertas, S. S. Senlik and A. Aydinli, *Opt. Express*, 2008, **16**, 12469.
14 X. N. Wang, Y. Y. Wang, M. Cong, H. B. Li, Y. J. Gu, J. R. Lombardi, S. P. Xu and W. Q. Xu, *Small*, 2013, **9**, 1895.
15 K. J. McKee, M. W. Meyer and E. A. Smith, *Anal. Chem.*, 2012, **84**, 4300.
16 S. A. Meyer, B. Auguie, E. C. Le Ru and P. G. Etchegoin, *J. Phys. Chem. A*, 2012, **116**, 1000.
17 H. B. Li, S. P. Xu, Y. Liu, Y. J. Gu and W. Q. Xu, *Thin Solid Films*, 2012, **520**, 6001.
18 M. Futamata, *Appl. Opt.*, 1997, **36**, 364.
19 T. H. Taminiau, F. D. Stefani and N. F. van Hulst, *Nano Lett.*, 2011, **11**, 1020.
20 Z. Zhang, A. Weber-Bargioni, S. W. Wu, S. Dhuey, S. Cabrini and P. J. Schuck, *Nano Lett.*, 2009, **9**, 4505.
21 J. J. Baumberg, T. A. Kelf, Y. Sugawara, S. Cintra, M. E. Abdelsalam, P. N. Bartlett and A. E. Russell, *Nano Lett.*, 2005, **5**, 2262.
22 H. B. Li, Y. J. Gu, H. Y. Guo, X. N. Wang, Y. Liu, W. Q. Xu and S. P. Xu, *J. Phys. Chem. C*, 2012, **116**, 23608.
23 T. H. Taminiau, F. D. Stefani and N. F. Van Hulst, *New J. Phys.*, 2008, **10**, 105005.
24 V. Giannini, A. I. Fernández-Domínguez, S. C. Heck and S. A. Maier, *Chem. Rev.*, 2011, **111**, 3888.
25 N. Bonod, A. Devilez, B. Rolly, S. Bidault and B. Stout, *Phys. Rev. B: Condens. Matter Mater. Phys.*, 2010, **82**, 115429.
26 A. Baron, E. Devaux, J. C. Rodier, J. P. Hugonin, E. Rousseau, C. Genet, T. W. Ebbesen and P. Lalanne, *Nano Lett.*, 2011, **11**, 4207.
27 J. H. Zhang, Z. Chen, Z. L. Wang, W. Y. Zhang and N. B. Ming, *Mater. Lett.*, 2003, **57**, 4466.
28 Y. F. Li, J. H. Zhang, S. J. Zhu, H. P. Dong, F. Jia, Z. H. Wang, Z. Q. Sun, L. Zhang, Y. Li, H. B. Li, W. Q. Xu and B. Yang, *Adv. Mater.*, 2009, **21**, 4731.
29 H. Raether, *Surface Plasmons on Smooth and Rough Surfaces and on Gratings*, Springer-Verlag, Hamburg, Germany, 1986, ch. 2.
30 T. W. Ebbesen, H. J. Lezec, H. F. Ghaemi, T. Thio and P. A. Wolff, *Nature*, 1998, **391**, 667.
31 Y. Liu, S. P. Xu, X. Y. Xuan, B. Zhao and W. Q. Xu, *J. Phys. Chem. Lett.*, 2011, **2**, 2218.

 This journal is © the Owner Societies 2013